AUTHOR QUERIES

AUTHOR PLEASE ANSWER ALL QUERIES

PLEASE NOTE: Please note that we cannot accept new source files as corrections for your article. If possible, please annotate the PDF proof we have sent you with your corrections and upload it via the Author Gateway. Alternatively, you may send us your corrections in list format. You may also upload revised graphics via the Author Gateway.

Carefully check the page proofs (and coordinate with all authors); additional changes or updates WILL NOT be accepted after the article is published online/print in its final form. Please check author names and affiliations, funding, as well as the overall article for any errors prior to sending in your author proof corrections. Your article has been peer reviewed, accepted as final, and sent in to IEEE. No text changes have been made to the main part of the article as dictated by the editorial level of service for your publication.

AQ:1 = Please confirm the representation of all the authors' name throughout the article.

AQ:2 = Please confirm whether the edits made in the current affiliation of all the authors are correct.

AQ:3 = Please confirm or add details for any funding or financial support for the research of this article.

AQ:4 = It was indicated that research for this article involved either human subjects or animals. Please provide the name of the Review Board or Committee approving the human/animal research for your article.

AQ:5 = If you haven't done so already, please make sure you have submitted a graphical abstract for your paper. The GA should be a current figure or image from your accepted article. The GA will be displayed on your articles abstract page on IEEE Xplore. Please choose a current figure from the paper and supply a caption at your earliest convenience for the graphical abstract. Note that captions cannot exceed 1800 characters (including spaces). If you submitted a video as your graphical abstract, please make sure there is an overlay image and caption. Overlay images are usually a screenshot of your video that best represents the video. This is for readers who may not have access to video-viewing software. Please see an example in the link below: http://ieeeaccess.ieee.org/submitting-an-article/

AQ:6 = Please confirm whether the placement of information in the Acknowledgment section is correct.

AQ:7 = Please provide the publisher name and publisher location for Ref. [4].

IEEE Access
Multidisciplinary ⋮ Rapid Review ⋮ Open Access Journal

Received 21 October 2024, accepted 11 November 2024. Date of publication 00 xxxx 0000, date of current version 00 xxxx 0000.

Digital Object Identifier 10.1109/ACCESS.2024.3498444

An Adaptation of Fitts' Law for Performance Evaluation and Optimization of Augmented Reality (AR) Interfaces

AQ:1 **ONYEKA JOSEPHINE NWOBODO [1], KAMIL WERESZCZYŃSKI [1], GODLOVE SUILA KUABAN [2], PRZEMYSŁAW SKUROWSKI [1], AND KRZYSZTOF ADAM CYRAN [1]**

AQ:2 [1]Department of Computer Graphics, Vision, and Digital Systems, Faculty of Automatic Control, Electronics and Computer Science, Silesian University of Technology, 44-100 Gliwice, Poland
[2]Institute of Theoretical and Applied Informatics, Polish Academy of Sciences, 44-100 Gliwice, Poland

Corresponding author: Onyeka Josephine Nwobodo (onyeka.nwobodo@polsl.pl)

AQ:3 This work was supported in part by the European Union's Horizon Europe Program under Grant 101080374-OptiQ, and in part by the Resources of the Polish Ministry of Science and Higher Education in a Frame of Program International Co-Financed Projects.

AQ:4 This work involved human subjects or animals in its research. Approval of all ethical and experimental procedures and protocols was granted by (Name of Review Board or Committee) (IF PROVIDED under Application No. xx, and performed in line with the (Name of Specific Declaration)).

AQ:5 **ABSTRACT** There is growing widespread adoption of augmented reality in tech-driven industries and sectors of society, such as medicine, gaming, flight simulation, education, interior design and modelling, entertainment, construction, tourism, repair and maintenance, public safety, agriculture, and quantum computing. However, ensuring smooth and intuitive interactions with augmented objects is challenging, requiring practical performance evaluation and optimization models to assess and improve users' experiences with AR-enhanced systems. In this paper, we apply Fitts' Law to model and predict interaction task difficulty with objects distributed across four spatial quadrants. We use genetic optimization algorithms to fine-tune Fitts' Law parameters, achieving a model that significantly enhances predictive accuracy. Our optimized model demonstrates an approximately 40% reduction in interaction task difficulty across all quadrants, leading to a more ergonomic and intuitive user interface. This study contributes to the Human-Computer Interaction (HCI) field by offering a refined metric for evaluating and optimizing AR interfaces and addressing the unique challenges of three-dimensional interaction environments. Therefore, we propose a practical framework for the performance evaluations and optimization of augmented reality and other user interfaces.

INDEX TERMS Augmented reality, SLAM, Fitts' law, level of difficulty, ergonomics in AR, user engagement.

I. INTRODUCTION

Augmented reality (AR) is revolutionizing how we engage with digital information systems by integrating virtual elements with the physical world [1], profoundly impacting various industries and sectors of society such as robotics, gaming, marketing, education, repair and maintenance, medicine, flight simulation, security and safety, interior design and modelling, construction, agriculture, and quantum computing. At the core of this technology is SLAM (Simultaneous Localization and Mapping), which leverages a combination of sensors, such as cameras and Inertial Measurement Units (IMUs), to ensure precise alignment of digital content within the user's real-world environment [2]. This precision enhances the immersive and engaging quality of AR interactions.

Despite the rapid advancements in AR technology, ensuring that these interactions are both ergonomic and intuitive

The associate editor coordinating the review of this manuscript and approving it for publication was Francesco Strada.

presents significant challenges. Developing robust interaction models that leverage natural gestures is essential for maximizing AR technologies' potential to create engaging user experiences. Research shows that effective user engagement strategies in AR can lead to better retention, enhanced learning outcomes, and higher satisfaction across various AR applications [3].

This paper addresses a critical gap in HCI research by adapting Fitts' Law—traditionally applied to two-dimensional (2D) interfaces for use in the complex, three-dimensional (3D) environments of AR. Fitts' Law predicts the time required to move to and select a target based on the target's distance and the target's size [4], which is essential in understanding and optimizing user interactions. By incorporating head movement and SLAM-based spatial awareness, this study contributes a novel approach to modelling and predicting interaction difficulties in AR, advancing the broader field of HCI. While a few studies (e.g., [5], [6]) have attempted to extend Fitts' Law to evaluate 3D virtual environments, considering performance metrics such as index of difficulty and movement time (MT), a critical challenge in AR lies in aligning user expectations with interaction outcomes. Discrepancies in this alignment can lead to decreased satisfaction and efficiency.

To address these challenges, our study incorporates a comprehensive survey that captures subjective user experiences with AR elements in different spatial orientations. This data, combined with experimental findings, validates the accuracy and robustness of our model. The contributions of this paper are summarized as follows:

- We evaluate the interaction task difficulty in various AR quadrant environments using the Fitts' Law framework.
- We refine Fitts' Law parameters specifically for AR interfaces, using a genetic optimization algorithm to enhance precision and usability in AR interactions.
- We established a benchmark for AR interaction models through a combination of subjective user surveys and experimental data, ensuring a thorough understanding of AR interface effectiveness.

The implications of our findings are profound, with the potential to influence a wide audience, including those involved in game development for VR and AR solutions, interactive applications—such as flight, optical, and car simulators—and service application creators. [7], [8]. This work is a pivotal step towards optimizing AR technology for practical use, providing professionals and researchers with the necessary insights and tools to shape the future of AR interfaces. It offers a promising outlook for the future of AR technology, where user-friendly and efficient interfaces are the standard.

II. RELATED WORK

Fitts' Law, a foundational concept in HCI, was initially developed for Graphical User Interfaces (GUIs) to predict the task difficulty of interacting with objects based on factors such as target shape and movement direction. This is particularly critical in augmented reality, where spatial properties like target distance, size, and user interaction dynamics play crucial roles [9]. Over the years, Fitts' Law has been adapted to various interfaces, including touchscreens [10], [11], [12] and Virtual Reality (VR) systems [13]. The evolution of Fitts' Law from 2D interfaces to its application in 3D virtual and augmented reality environments represents a significant milestone in Human-Computer Interaction (HCI).

This evolution began with MacKenzie and Buxton's seminal work in 1992, which extended Fitts' Law to 2D mouse-based pointing tasks [14]. 2003 Accot and Zhai refined this model for 2D interfaces by incorporating a weighted Euclidean norm to improve target acquisition predictions [15]. These early adaptations laid the groundwork for more sophisticated interactions across different dimensions. In 2001, Murata and Iwase introduced the first significant adaptation of Fitts' Law to 3D interfaces by incorporating azimuth angles to predict user performance in 3D spaces [16]. This was followed by Grossman and Balakrishnan's 2004 model, which integrated variables such as target size and movement direction within 3D environments [17]. Subsequent advancements, such as those by Cha and Myung in 2013, who focused on spherical targets and inclination angles [18], and Schuetz et al. in 2019, who emphasized gaze-based interactions in 3D spaces [19], have further refined the application of Fitts' Law in complex interaction scenarios.

Recent studies have continued this trend of refinement. For instance, Jiang and Gu provided an extensive review of modern adaptations of Fitts' Law across various platforms, including its application to three-dimensional Human-Computer Interactions (HCI) and augmented reality environments [12]. Clark, Bhagat, and Riggs in 2020 explored the application of Fitts's Law in VR using low-cost technology [5], while Lou et al. in 2021 examined hand-adaptive interfaces in VR [20]. Liu et al. [21] explored the study of rotation gestures on touchscreens enhanced with electrostatic tactile feedback. They demonstrated that adding tactile feedback, either in the target area or during the interaction process, significantly improves the efficiency and accuracy of rotation operations, adhering closely to Fitts' Law [21]. Wagner et al. [22] studied gaze-hand alignment in 3D user interfaces, comparing techniques like Gaze&Finger and Gaze&Handray against hand-only methods. Their findings showed that gaze-hand techniques outperformed the baselines, especially for targets close to the image plane, with reduced performance at greater depths due to parallax effects [22].

However, applying Fitts' Law to AR remains underexplored, particularly in environments where head movement and spatial orientation play critical roles. Existing adaptations often do not sufficiently account for the nuances of AR, where the user's physical orientation and the dynamic nature of the environment significantly impact interaction task difficulty.

This paper builds on the work of MacKenzie and Buxton [14] and others who have extended Fitts' Law to 2D and 3D environments. To address this gap, we propose a model that integrates head movement and SLAM-based spatial awareness into Fitts' Law, offering a refined model that specifically addresses the unique challenges posed by AR.

III. METHODOLOGY

Our study adapts Fitts' Law to the unique demands of AR environments by integrating head movement into the model and refining key parameters using a genetic optimization algorithm.

A. ERGONOMIC INTERACTIVE ELEMENT PLACEMENT IN AR

Our research investigates the application of Fitts' Law to analyze user interactions within various quadrants of a 360° AR environment [23]. This analytical approach allows us to understand and quantify the ease with which users can locate and engage with objects contextually instantiated within their virtual space, corresponding to the cardinal and intercardinal directions outlined in figure 1.

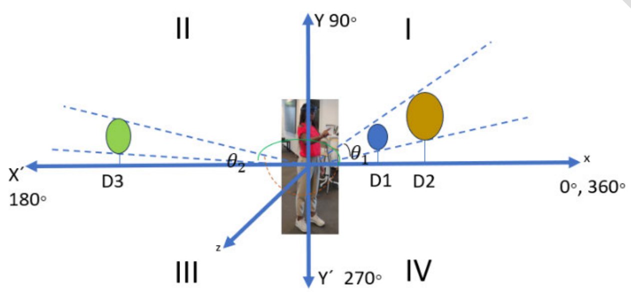

FIGURE 1. Ergonomic placement and angular interaction framework for AR objects: This schematic depicts the strategic positioning of interactive objects within a user's 360° field in an AR environment, highlighting the angular dimensions and ergonomic zones that facilitate intuitive interaction.

We leverage Unity's XR Interaction Toolkit to position interactive elements within the AR environment strategically. Based on spherical coordinates, this positioning adheres to specific ergonomic zones designed for user comfort and interaction efficiency [24]. Our approach extends the traditional application of Fitts' Law, emphasising the impact of target proximity and size on interaction time. We adapt this law to the three-dimensional AR context, where user accessibility and field of view are crucial factors. Beyond varying object scales and colours, we strategically place them to align with natural human gaze and movement patterns, similar to recent work highlighting the importance of ergonomic design in enhancing AR interaction [25]. Segmenting the user-centric space into anatomical planes (akin to Figure 2) provides a nuanced understanding of spatial interaction in AR. This segmentation allows us to identify areas of varying interaction task difficulty based on ergonomic limitations. Our findings indicate that initial user engagement often focuses on the upper frontal quadrant, suggesting potential strain due to ergonomic limitations. This aligns with research emphasizing the importance of aligning virtual objects with natural ergonomic boundaries to minimize user strain and improve interaction quality [26].

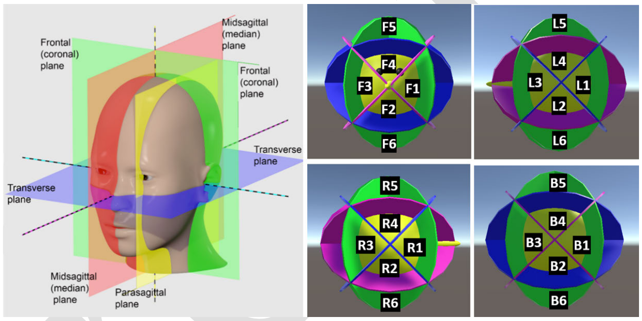

FIGURE 2. Anatomical planes and AR interaction zones for ergonomic interface design: This illustration juxtaposes the division of the human body by anatomical planes (left) [26] with their application in AR interaction zones (right), delineating quadrant-based zones for intuitive user engagement. It is a visual framework for designing AR interfaces that complement natural human movement patterns.

B. SLAM-BASED SPATIAL ANCHORING IN AR OBJECT INTERACTION

Algorithm 1 outlines our novel approach for dynamically placing various 3D models within an AR environment. Leveraging the HoloLens' Simultaneous Localization and Mapping (SLAM) capabilities and spatial awareness toolkit, the algorithm continuously tracks the user's environment, forming the foundation for anchoring virtual objects. The algorithm initializes the SLAM system, establishing a real-time map of the user's surroundings. Subsequently, it determines the number (N) of objects to be instantiated within the AR scene. Each object type is intelligently selected from a pre-defined set, ensuring diverse user experiences.

The algorithm uses the Spatial Awareness system to identify suitable placement locations within the user's current environment. These locations consider the user's position, environmental obstacles, and ergonomic factors, ensuring object placement within reachable and visible zones. Spherical coordinates are then computed for each object relative to the user and converted into Cartesian coordinates based on the HoloLens' spatial understanding. This step guarantees object positioning within the user's field of view and at suitable interaction distances, enhancing immersion and interaction comfort. Also, each object is instantiated at the calculated position with randomly applied scaling and colour. This variability promotes user engagement and allows for assessing the impact of object appearance on interaction. As users interact with the objects, vital metrics are collected throughout the session. After completion, the SLAM system concludes the session, and the collected data is saved for further analysis. More details about the implementation and analysis can be found in GitHub.

Algorithm 1 AR Object Placement and Interaction Data Collection

Require: C: CameraPosition ▷ The position of the AR camera in world space
Require: r: $[r_{\min}, r_{\max}]$ ▷ Range of distances for object placement
Require: O: [Sphere, Cube, Car] ▷ Array of 3D object prefabs
Ensure: L: [] ▷ List to store instantiated objects and their properties

InitializeCamera(C) ▷ Set up the AR camera at position C
$N \leftarrow$ DetermineSampleCount() ▷ Determine the total number of samples required
for $i \leftarrow 1$ to N **do**
    $T \leftarrow$ SelectRandomObject(O) ▷ Select an object type at random from O
    $[H, V] \leftarrow$ [SelectRandomHorizontalQuadrant(), SelectRandomVerticalQuadrant()] ▷ Select horizontal and vertical placement quadrants randomly
    $[d, \theta, \phi] \leftarrow$ [GenerateRandomDistance(r), CalculateAngle(H), CalculateAngle(V)] ▷ Generate spherical coordinates
    $[x, y, z] \leftarrow [d \cdot \sin(\phi) \cdot \cos(\theta), d \cdot \sin(\phi) \cdot \sin(\theta), d \cdot \cos(\phi)]$ ▷ Convert spherical coordinates to Cartesian coordinates
    $P \leftarrow C + [x, y, z]$ ▷ Calculate the object's world position relative to the camera
    SetObjectPosition(T, P) ▷ Set the object's position to P
    $[S, Col] \leftarrow$ [GenerateRandomScale(), GenerateRandomColor()] ▷ Generate random scale and color
    ApplyTransformations(T, S, Col) ▷ Apply the transformations to the object
    L.Add(T, CaptureMetrics(P, S, Col)) ▷ Add object and metrics to the list
    HandleUserInteraction(T) ▷ Handle user interaction with the object T
    $[Att, \Omega] \leftarrow$ CaptureInteractionMetrics(T) ▷ Record interaction time and orientation
    $N \leftarrow N - 1$ ▷ Decrement the sample count
    SaveData(L) ▷ Persist the collected data to storage
end for
if $N = 0$ **then**
    TerminateExperiment() ▷ Conclude the experiment and clean up resources
end ifreturn L ▷ Return the list of instantiated objects and their properties

C. ADAPTATION OF Fitts' LAW INTO AR ENVIRONMENT

In augmented reality (AR) interactions, multiple factors influence the task difficulty. In this study, we utilize several difficulty metrics to evaluate AR interactions:

1) INDEX OF DIFFICULTY (ID)

Based on Fitts' Law, ID quantifies interaction difficulty using target size and distance.

2) LEVEL OF DIFFICULTY (LoD)

A novel metric we introduced, which adjusts for angular distances between the user and AR objects, providing a refined measure of spatial interaction complexity.

3) TASK DIFFICULTY

A general term referring to user-perceived or actual difficulty during AR interactions influenced by both ID and LoD. Throughout this paper, we specify which metric is being referenced to ensure clarity.

Traditional Fitts' Law models index of difficulty based on target distance and size. However, these factors alone are insufficient in AR environments, where users must often rotate their heads to align with targets. We propose a new index of difficulty (I_{3D}) that includes a head distance metric $d_m(H, T)$ calculated using quaternion algebra to account for head rotation and spatial positioning. Our genetic algorithm optimizes four key parameters: Λ (scaling factor), μ (optimal head distance), σ (width of head distance influence), and s (strength of head influence), to tailor the model to AR's specific needs, as described in Equation 6.

Originally, Fitts' Law was articulated as follows:

$$\mathcal{I}_D(S, T) = \log_2 \left[2 \frac{d(S, T)}{w(T)} \right] \tag{1}$$

where $\mathcal{I}_D(S, T)$ represents the index of difficulty between a source object (S) and a target object (T), with $d(S, T)$ being the distance between them and $w(T)$ denoting the width of the target object. Furthermore, the index of performance (IP) is defined as:

$$\mathcal{I}_P(S, T) = \frac{\mathcal{I}_D(S, T)}{\delta t(S, T)} \tag{2}$$

with $\delta t(S, T)$ indicating the time taken to move from the source to the target object [14].

In the context of AR, as experienced through Hololens, traditional metrics like Euclidean distance and object width become less significant. This is due to the unique spatial interactions in AR, where the user's physical orientation and position play a critical role. We observed that interactions involving head or body rotation present a different challenge, particularly when objects are positioned at unconventional angles or near the user. "With head movement" refers to scenarios where the user needs to move their head to align their gaze with the target, thereby influencing the task's difficulty. Conversely, "without head movement" refers to interactions where the user's head remains stationary and only the hand or controller moves to interact with the target. Such spatial arrangements necessitate modifying the original Fitts' Law to accurately reflect the complexities of AR interactions.

To address these challenges, we incorporated the concept of quaternion algebra to represent head rotation. The rotation of a vector p, defined as a unit quaternion, by a rotation quaternion q is given by:

$$p' = q \cdot pq^{-1} \tag{3}$$

where $q^{-1} = q^*$ represents the conjugate of q. This approach is substantiated by the work of Świtonski et al. [27], who provided a formula for calculating the distance in quaternion space:

$$d_Q(q_1, q_2) = \arccos(2\langle q_1, q_2\rangle - 1) \tag{4}$$

This formula captures the rotational distance between two quaternions, q_1 and q_2.

In adapting Fitts' Law for the 3D AR environment, we replaced the traditional width metric with the object's volume $V(T)$. We also introduced the head distance, $d_m(H, T)$, defined as the modified distance from the target object T to the user's head position H. The head distance is pivotal, especially when objects are close to the user, as these situations may complicate perception and interaction. Our hypothesis posits that task difficulty increases when this distance surpasses the threshold μ (in meters), which represents the point of optimal task difficulty, as visually depicted in Figure 3. The task difficulty is least when $d_m(H, T)$ is equal to μ, and it increases as the distance decreases, indicating that objects too close to the user may be challenging to interact with. This is particularly true for objects placed such that they require significant head movement to be perceived.

PARAMETERS IN THE MODIFIED FITTS' LAW

The head distance is mathematically expressed as:

$$d_m(H, T) = s - (s-1) \cdot e^{-\frac{1}{2}\left(\frac{d_Q(H,T)-\mu}{\sigma}\right)^2} \tag{5}$$

where s **(Strength of Head Influence)**: This parameter represents the strength of head movement's impact on interaction task difficulty. It is computed by analyzing head movement data captured via the HoloLens sensors. By measuring the amount of head rotation needed to align with each target, we quantify the extent to which head orientation increases task difficulty. This value is optimized using a genetic algorithm to minimize task completion time.

μ **(Optimal Head Distance)**: The parameter μ represents the optimal head distance, which is the distance at which interaction task difficulty is minimized. It is determined by analyzing the task completion times at various distances between the head and the target object.

σ **(Width of Head Distance Influence)**: This parameter defines the range of distances within which head movement significantly influences interaction task difficulty. The influence is modelled as a Gaussian distribution centred around μ, and σ represents the spread of this influence.

These parameters, s, μ, and σ, are empirically determined through experiments, as illustrated in Figure 3. They are refined through a genetic optimization algorithm to tailor the model to AR environments.

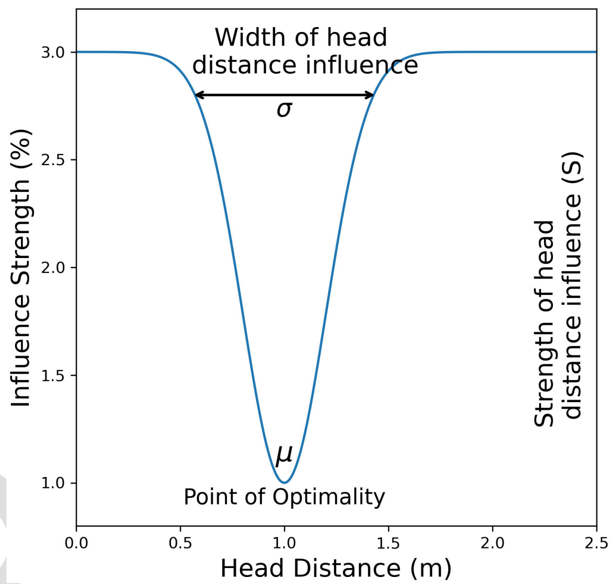

FIGURE 3. Illustration of the head distance influence with parameters s, μ, and σ.

Consequently, we have formulated a revised equation for the index of difficulty in a 3D AR environment, taking into account head rotation and object volume:

$$\mathcal{I}_{3D}(S, T) = \log_2\left[\Lambda \cdot d_m(H, T) \cdot \frac{d(S, T)}{V(T)}\right] \tag{6}$$

where $d(S, T)$ is the Euclidean distance between the source and target, and $V(T)$ is the volume of the target object. Although the index of performance (IP) formula remains unchanged, it now employs the revised index of difficulty I_{3D}. This adjustment to Fitts' Law offers a refined metric for evaluating the interaction intricacies in AR environments, as seen with Hololens usage.

D. OPTIMIZING Fitts' LAW PARAMETERS FOR AR

Our experimental design focuses on calibrating four pivotal coefficients in the revised Fitts's law: Λ, μ, s, σ. We introduce a quantified Level of Difficulty (LoD), as visually indicated in Figure 3, based on the normalized angular distance between the source and target objects, with normalization done by π to confine values within the [0, 1] interval. The LoDs are discretized into four categories:

$$\begin{aligned}
LoD = 1 &\Leftrightarrow 0.00 \leq d_m(H, T)/\pi < 0.25 \\
LoD = 2 &\Leftrightarrow 0.25 \leq d_m(H, T)/\pi < 0.50 \\
LoD = 3 &\Leftrightarrow 0.50 \leq d_m(H, T)/\pi < 0.75 \\
LoD = 4 &\Leftrightarrow 0.75 \leq d_m(H, T)/\pi \leq 1.00
\end{aligned} \tag{7}$$

Each experimental sample was assigned an initial LoD, which informed the subsequent calculation of the Index of Performance (IP) under two conditions: with and without the influence of head distance. Then, we divided the samples into groups according to LoD, and for each group, we calculated the mean and standard deviation. The range for the j-th group was defined as:

$$R(j) = \left[\text{avg}(LoD = j) - \text{std}(LoD = j), \text{avg}(LoD = j) + \text{std}(LoD = j)\right] \tag{8}$$

The calibration aims to satisfy two stringent conditions: firstly, that there is a marked and increasing separation between the average LoDs–specifically $avg(LoD = 1) \ll avg(LoD = 2) \ll avg(LoD = 3) \ll avg(LoD = 4)$ and secondly, that there is minimal or no overlap between the ranges of consecutive LoD groups, $R(j) \cap R(j+1)$, to ensure distinct differentiation between levels of difficulty.

IV. EXPERIMENTAL SETUP

The experiment was conducted using Microsoft HoloLens 2, a widely recognized AR device, to ensure the accuracy and relevance of the findings. The selection of HoloLens 2 was based on its robust sensor suite, which includes advanced head tracking capabilities essential for assessing head movement impacts on interaction task difficulty.

A. EXPERIMENTAL PROCEDURE

1) PARTICIPANT RECRUITMENT AND SELECTION

Thirty participants (24 males, 6 females, aged 18 to 50, mean = 32, SD = 13.39) were recruited using a multi-channel approach to ensure a representative sample across age, gender, and AR experience levels. This strategy was designed to capture diverse interaction patterns within the AR environment.

2) INFORMED CONSENT PROCESS

An exhaustive informed consent process was conducted in adherence to ethical standards and institutional guidelines, ensuring participants were fully briefed on the study's scope, involvement, potential risks, and rights, including confidentiality and voluntary participation.

3) TASK DESCRIPTION

Participants were categorized into two groups based on their posture—standing or seated—for the study, as depicted in Figure 4. They were equipped with the Microsoft HoloLens 2 and immersed in an AR-enabled environment optimized for interactive tasks. The procedure began with participants completing a registration form, where they provided their username, session ID, and the number of samples they would interact with during the session. Each session lasted approximately 10-15 minutes, depending on the number of samples selected. Participants with more AR experience typically selected more samples (40-60 samples), while those with less experience chose fewer (10-30 samples). No breaks were provided during the session to maintain participant engagement and ensure consistency in the data collection process.

After registration, a guiding arrow in their field of view directed attention towards a designated holographic target. These objects were placed at varying distances—ranging from 0.3 to 6.0 meters—from the participant and distributed across different quadrants in the AR environment to ensure spatial variation and engagement of head movement in different ergonomic directions. The objects themselves varied in size from 0.1 to 1.2 meters, with scaling factors applied between 0.3 and 0.5 for diversity, ensuring that participants encountered objects of different sizes and distances to interact with.

To maintain continuity, the guiding arrow's orientation was adjusted after each interaction to highlight the next target, with a two-second intermission and a message preparing participants for the following tasks. The array of holographic objects encountered—spanning spheres, cubes, and cars—was strategically varied to examine the impact of object form and participant posture on interaction modalities and user experience insights.

4) DATA

In our dataset, precisely recorded via the software mentioned above, each entry encapsulates the object's location and the observer's head orientation (both position and rotation) and quantifies the distortion vector's scale factor alongside the action's timing. The distortion vector meticulously records the object's scaling across various axes, adhering to a predefined range of [0.8, 1.2] to preserve the object's geometric integrity. We rigorously calculate the object's volume from this vector, ensuring a precise understanding of its spatial dimensions. Furthermore, the 'action time'—the interval from application initiation to the user's interaction with the object—is meticulously recorded. This time-based measurement, δt, crucial for computing the index of performance (referenced as eq.2), is derived by calculating the time difference between successive actions, adjusted by a two-second standard interval to account for experiment consistency. This detailed data collection and analysis framework underpins our experimental investigation, enabling a nuanced exploration of user interaction dynamics within AR environments. The data set comprises 659 samples (438 for standing and 221 for sitting cases). The division into the LoD is presented in Table 1 below.

TABLE 1. Data set characteristics. The number of samples and division into sitting and standing cases (horizontally) and into the level of difficulty (vertically).

No	Conditions	LoD=1	LoD=2	LoD=3	LoD=4	Total
1	Sitting	95	60	46	20	221
2	Standing	150	108	92	88	438
	Total	245	168	138	108	659

V. RESULTS AND DISCUSSION

Our refined model significantly improves the predictive accuracy of AR interactions, as demonstrated by a strong

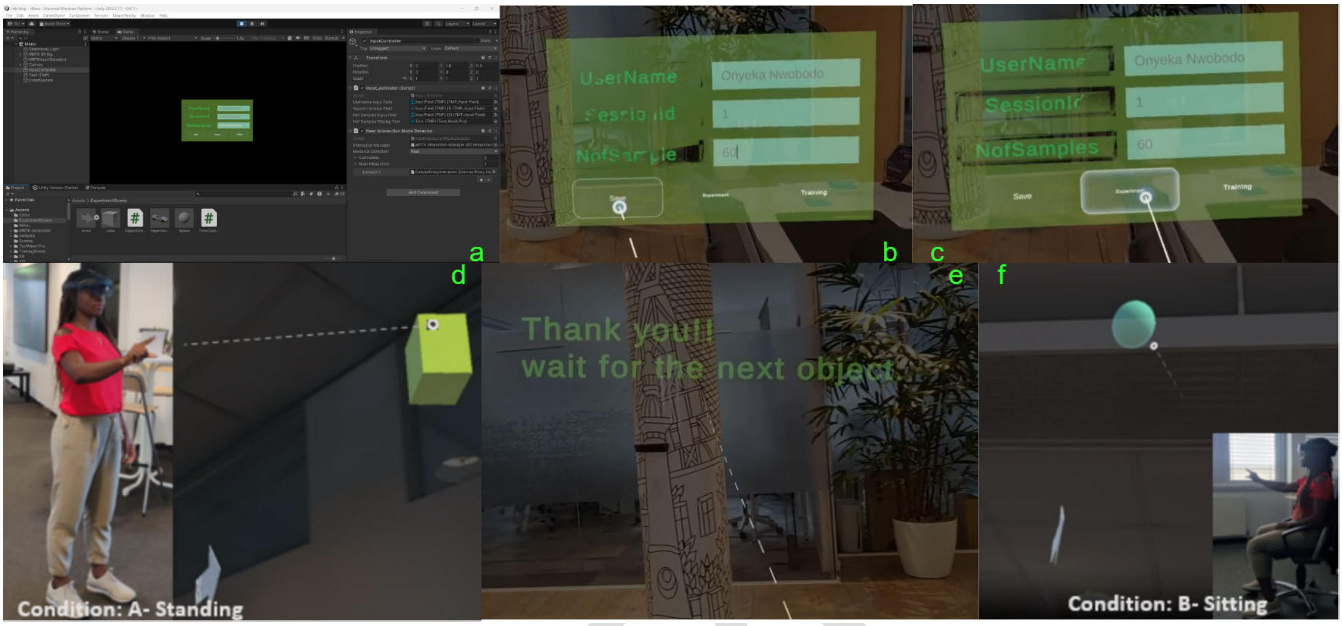

FIGURE 4. **Experiment setup: A user interacts with a virtual environment through a HoloLens device, performing tasks in both standing (Condition A panel(d)) and sitting (Condition B panel(f)) positions. The setup includes interface development in Unity panel(a), user input registration panel(b,c), and interaction with virtual objects panel (e).**

correlation ($R^2 = 0.910$) between the predicted and actual user performance data, as illustrated in Figure 12. A QQ plot (Figure 13) further confirms that the residuals follow a normal distribution, validating the model's predictive power across different interaction scenarios. By applying a genetic optimization algorithm to fine-tune key parameters of the modified Fitts' Law (I3D)—such as μ (optimal head distance), σ (width of head distance influence), and s (strength of head influence)—we achieved a 40% reduction in interaction task difficulty across various spatial quadrants. This reduction was measured against the initial interaction task difficulty values calculated using the modified Fitts' Law before applying optimization.

The 40% improvement is particularly notable in the upper frontal quadrant, where ergonomic challenges are most pronounced. The results were validated through empirical data collected from a flight simulation scenario, which closely mirrors real-world AR applications. The consistency of our findings across different spatial orientations underscores the robustness of the proposed model in predicting AR interaction challenges.

The spatial positioning of objects greatly influences interaction task difficulty. Objects within the user's direct line of sight (0° to 90°) are more accessible to interact with, while those positioned outside this range require more complex movements. Our detailed examination of these interaction challenges within the AR setting is documented in Tables 2 (standing), 3 (sitting) and illustrated in Figure 7. These results outline the average and standard deviation of the Index of Difficulty (ID) across various conditions.

In addition to the spatial analysis, we assessed the distribution of absolute errors across the four quadrants in both standing and sitting conditions. As shown in Figure 8, the standing condition exhibits a higher spread of absolute error in the first and fourth quadrants (Q1 and Q4), indicating increased task difficulty in these regions. This variability is likely due to the ergonomic challenges associated with these spatial orientations, particularly those outside the user's direct line of sight. In contrast, the absolute errors across quadrants in the sitting condition were more consistent, with less variability than in the standing condition. This consistency suggests that users can better manage interactions across the quadrants while sitting due to increased stability and reduced physical strain. This segmentation by quadrant highlights how spatial orientation affects interaction task difficulty and emphasizes the importance of head orientation.

A. STATISTICAL ANALYSIS

We conducted repeated-measures ANOVAs with Tukey HSD post hoc tests at the 5% significance level. Normality was confirmed via QQ plots (Figure 13), showing that the residuals followed a normal distribution. The ANOVA revealed a significant main effect of target location on task difficulty for both standing and sitting conditions ($F(3, N) = 46.51$, $p < 0.001$). Post-hoc tests identified significant differences between Q1, Q2, and Q4 for standing, and Q1 and Q3 for sitting as illustrated with an asterisk in (Figure 7).

Despite these differences, the error results (STD) in Figure 8 showed no significant differences in performance variability between quadrants for either condition

(F(3, N) = 1.53, p = 0.257), indicating similar consistency across all quadrants.

Post-optimization, a significant main effect was observed for both conditions ($F(3, N) = 148.99$, $p < 0.001$) (Figure 15). Post-hoc tests showed significant differences in task difficulty for Q1 and Q4 in standing and Q1 and Q3 in sitting.

1) LIGHTING CONDITION ANALYSIS

We also analyzed how lighting conditions impacted task difficulty across different spatial quadrants in both standing and sitting positions. Brightness levels were categorized into three groups: low, medium, and high, and the Index of Difficulty (IoD) was analyzed using ANOVA and post-hoc Tukey HSD tests. The ANOVA revealed a significant effect of brightness on task performance ($F = 4.16$, $p = 0.016$), indicating that changes in brightness levels notably influenced task performance. Tukey HSD further identified Quadrant 4 as being most affected by brightness, with high brightness leading to increased task difficulty (F-statistic: 3.37, p-value: 0.038). Figure 5 illustrates this relationship, with asterisks marking the significant impact in Quadrant 4. This suggests that visual strain or ergonomic factors may play a role in heightened task difficulty in this quadrant.

In contrast, the sitting condition did not show a significant effect of brightness on task difficulty ($F = 0.581$, $p = 0.560$). Task difficulty remained consistent across brightness levels in the sitting condition, as shown in Figure 5. These findings suggest that standing tasks, particularly in Quadrant 4, are more sensitive to lighting while sitting tasks are less affected.

2) ENVIRONMENTAL COMPLEXITY IN AR

To assess environmental complexity in the augmented reality (AR) setting, we analyzed two factors: crowding (object count within quadrants) and object positioning (horizontal and vertical). Task difficulty was measured through interaction time, and ANOVA tests evaluated these factors. Objects were categorized into low, medium, and high levels of crowding. The ANOVA did not show a significant effect of crowding on task difficulty ($F = 3.52$, $p = 0.0602$).

The ANOVA test for object positioning revealed that horizontal placement significantly impacted task difficulty ($F = 10.73$, $p = 0.0025$), while vertical placement did not ($F = 1.56$, $p = 0.2658$). Post-hoc Tukey HSD identified a significant difference between HQuadrants 2 and 4 ($p = 0.024$). Figure 6 illustrates these effects, emphasizing the role of horizontal positioning in driving task performance challenges.

This highlights the importance of optimizing lighting conditions and spatial organization, especially for standing work tasks, to reduce visual fatigue and improve performance.

To further illustrate user task difficulties, we present an integrated perspective on interaction complexity, merging assessments from horizontal and vertical planes to capture the multifaceted nature of AR experiences. This synthesis allows for a thorough evaluation of the ergonomic and cognitive load on users across different spatial orientations, enhancing our

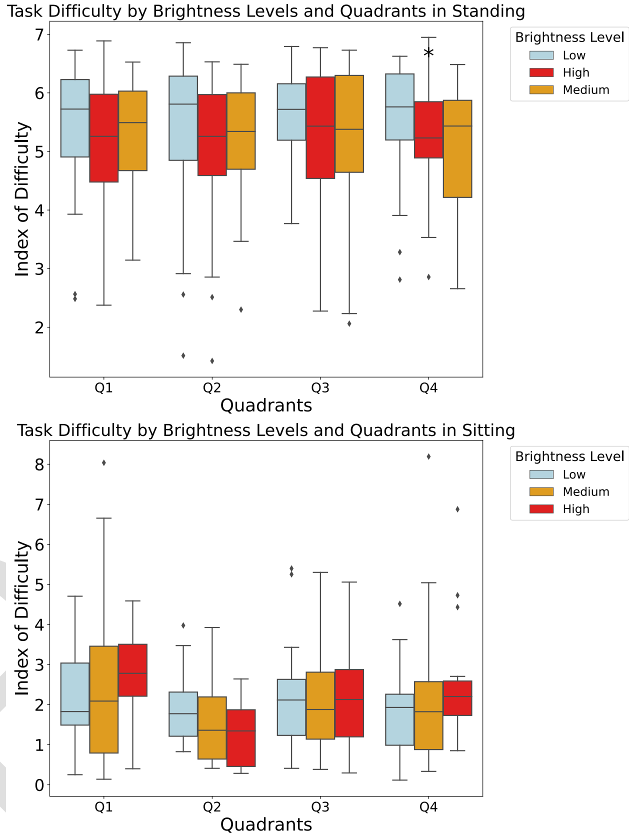

FIGURE 5. **The Figure compares the Index of Difficulty (IoD) across four quadrants (Q1 to Q4) under three brightness levels (Low, Medium, and High) for both standing (top) and sitting (bottom) conditions. The asterisks (*) in the standing condition indicate significant differences in task difficulty (p < 0.05), with Quadrant 4 showing the greatest sensitivity to high brightness levels.**

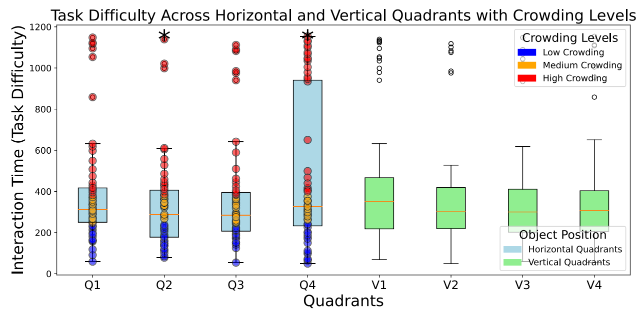

FIGURE 6. **Boxplots show task difficulty (interaction time) across horizontal (Q1–Q4) and vertical (V1 – V4) quadrants under different crowding levels (Low, Medium, High). Object positioning includes both horizontal and vertical quadrants. Asterisks (*) indicate significant differences in task difficulty for horizontal quadrants (p < 0.05), particularly in Q2 and Q4.**

model's utility and informing the design of user-centric AR interfaces.

In the intricate three-dimensional environment of AR, evaluating task difficulty requires a holistic approach that considers the full scope of user interactions. Our research introduces a comprehensive metric that integrates horizontal

TABLE 2. The Average (AVG) and Standard Deviation (STD) of task difficulty measures in standing conditions (Horizontally and Vertically) without and with head influence.

	Q1		Q2		Q3		Q4	
	HLoD	VLoD	HLoD	VLoD	HLoD	VLoD	HLoD	VLoD
Without Head Influence								
AVG	1.122	1.098	0.911	0.918	0.951	0.927	1.112	1.200
STD	0.733	0.695	0.566	0.633	0.685	0.652	0.856	0.897
With Head Influence								
AVG	1.534	1.503	1.264	1.255	1.288	1.339	1.512	1.643
STD	0.945	0.906	0.769	0.835	0.912	0.912	1.089	1.162

TABLE 3. The Average (AVG) and Standard Deviation (STD) of task difficulty measures in sitting conditions (Horizontally and Vertically) without and with head influence.

	Q1		Q2		Q3		Q4	
	HLoD	VLoD	HLoD	VLoD	HLoD	VLoD	HLoD	VLoD
Without Head Influence								
AVG	1.971	1.765	1.450	1.649	1.955	2.019	2.224	2.094
STD	1.329	1.110	0.844	0.948	1.133	1.203	1.370	1.414
With Head Influence								
AVG	2.337	2.068	1.720	1.946	2.296	2.369	2.620	2.494
STD	1.581	1.327	1.003	1.130	1.382	1.407	1.609	1.707

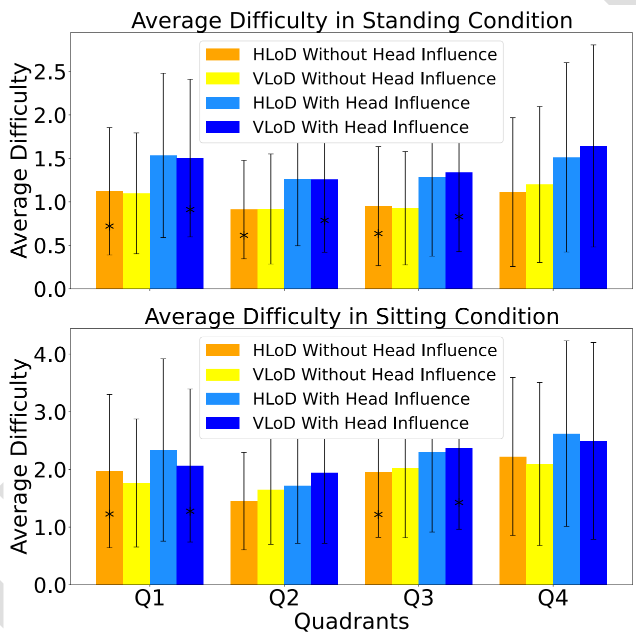

FIGURE 7. The bar charts show the average perceived task difficulty of AR interactions while standing and sitting across four quadrants (Q1-Q4), both with and without head movement. The asterisks (*) indicate quadrants with statistically significant differences ($p < 0.05$). These charts highlight increased task difficulty with head movement, emphasizing the importance of ergonomic design in AR interfaces.

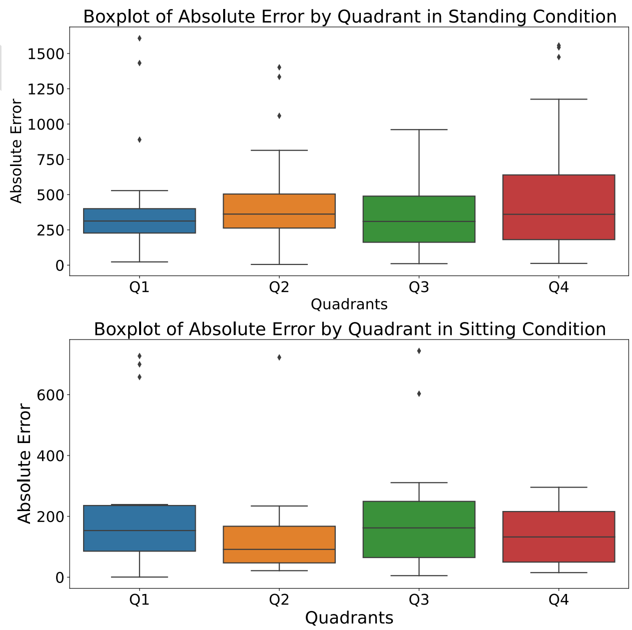

FIGURE 8. This figure shows the absolute errors across four quadrants (Q1 to Q4) during AR interactions in standing (top) and sitting (bottom) conditions. Each boxplot displays the error variability, with outliers marked as points, highlighting the precision and consistency of interactions across the conditions.

and vertical dimensions using the cosine and sine of user movement angles as indicators. The quadrant-specific behavior of cosine and sine functions is foundational to this approach, as detailed in Table 4, which defines the angle ranges for different quadrants and provides the necessary conditions for determining which quadrant each interaction belongs to. This is particularly important in spatial navigation within AR, where user movements can vary across horizontal and vertical axes.

To quantify task difficulty in these contexts, the task difficulty metric D_Q for each quadrant Q is formulated as:

$$D_Q = \sqrt{(\cos_{AVG})^2 + (\sin_{AVG})^2} \tag{9}$$

This equation is based on the standard 2D Euclidean norm, which combines the squared cosine and sine values representing user movement's horizontal and vertical components. These components reflect the relative task difficulty performed in the different quadrants. Each trigonometric component maps to a quadrant as indicated in Table 4, enabling us to assess the overall interaction task difficulty based on user movement direction.

Given that AR interactions occur in a three-dimensional space, our methodology adapts this 2D metric to suit the 3D context. We do this by normalizing the task difficulty metric across all quadrants. This normalization is essential to ensure that interaction task difficulty is represented consistently across different spatial dimensions, avoiding bias introduced by quadrant-specific complexities.

To achieve this, we normalize the metric to a 0-1 scale by dividing by the maximum value of $\sqrt{2}$, which is the upper bound of the Euclidean norm in a 2D space when both horizontal and vertical components contribute equally. This ensures that the task difficulty metric reflects the same range of values across different conditions:

$$D_{Q_{\text{norm}}} = \frac{D_Q}{\sqrt{2}} \tag{10}$$

Our methodology effectively combines user interaction's horizontal and vertical aspects into a single measure of task difficulty, offering a powerful tool for assessing AR performance. Integrating these multidimensional interactions into a comprehensive task difficulty metric, as shown in Equation 9, provides a transparent and standardized way to evaluate user challenges in AR environments. The result is illustrated in Figure 9.

B. QUANTITATIVE EVALUATION OF USER INTERACTION CHALLENGES

We employed a Weighted Average Difficulty (WAD) metric derived from user ratings to assess the perceived task difficulty of interacting with AR targets. This metric, detailed in Table 5 and illustrated in Figure 11, was calculated using the formula:

$$WA = \sum_{i=1}^{n} (P_i \times V_i) \tag{11}$$

whereP_i represents the percentage of responses for level of difficulty i, and V_i corresponds to the ordinal value assigned (1 to 7, from "Very Easy" to "Extremely Hard"). This approach ensures a proportional reflection of perceived task difficulty. Our analysis of the WAD across different task series revealed moderate variance in the F Series (2.38 to 4.35), with F4 being notably challenging. The L Series exhibited a narrower level of difficulty range, peaking at 5.29 for L6. The R Series was consistently challenging, with R6 having the highest level of difficulty (5.36). The B Series displayed the broadest range, with B6 being the most demanding (5.50). We observed patterns in WAD values, such as identical ratings for L4 and R3/R4 (3.34 and 3.71), respectively, and extreme values–B6 being the most challenging and F3 being the least. These insights informed our computational analysis and interface design.

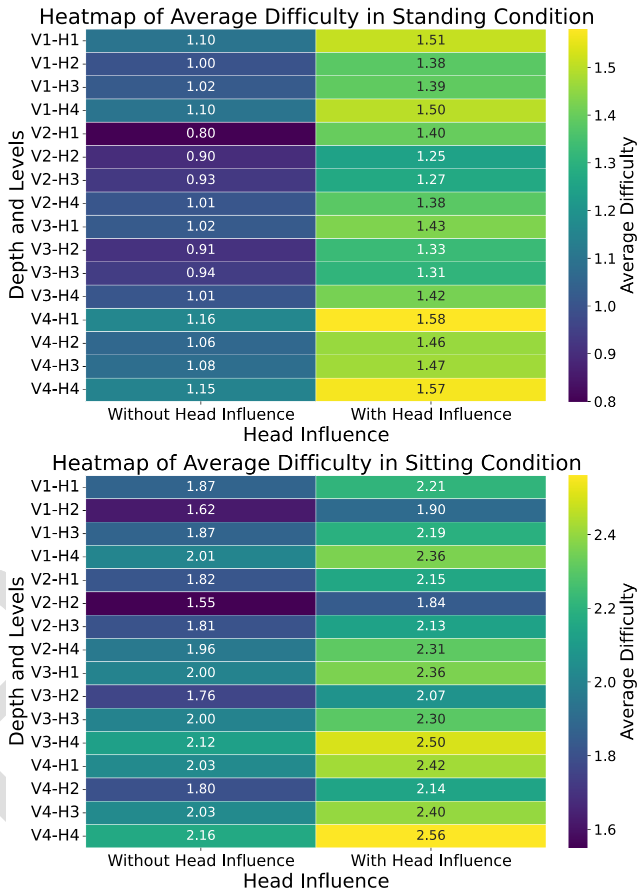

FIGURE 9. Heatmaps of AR interaction task difficulty: These heatmaps visually contrast average task difficulty in standing and sitting positions, with (right) and without (left) head movement. Colour gradients indicate the level of difficulty, with lighter shades denoting higher challenges. They emphasize how head movement increases the task difficulty, informing ergonomic AR design.

TABLE 4. Trigonometric conditions for quadrant determination.

Condition	Range of y
If $\cos y > \frac{1}{\sqrt{2}}$ and $\sin y \in \left[-\frac{1}{\sqrt{2}}, \frac{1}{\sqrt{2}}\right]$	$[0, \frac{\pi}{4}]$
If $\sin y > \frac{1}{\sqrt{2}}$ and $\cos y \in \left[-\frac{1}{\sqrt{2}}, \frac{1}{\sqrt{2}}\right]$	$[\frac{\pi}{4}, \frac{3\pi}{4}]$
If $\cos y < -\frac{1}{\sqrt{2}}$ and $\sin y \in \left[-\frac{1}{\sqrt{2}}, \frac{1}{\sqrt{2}}\right]$	$[\frac{3\pi}{4}, \frac{5\pi}{4}]$
If $\sin y < -\frac{1}{\sqrt{2}}$ and $\cos y \in \left[-\frac{1}{\sqrt{2}}, \frac{1}{\sqrt{2}}\right]$	$[\frac{5\pi}{4}, \frac{7\pi}{4}]$

To validate these findings, vector data from a Hololens experiment was incorporated into Unity, aligning with interaction quadrants shown in Figure 10. This spatial mapping of user interactions confirmed that certain quadrants, like the upper frontal area, presented higher level of difficulty, consistent with our earlier results. Our comprehensive analysis strongly supports the robustness and applicability of our optimized Fitts' Law model in real-world AR environments.

IEEE Access

This reassures us and our audience of the validity of our findings and the potential of Fitts' Law in understanding user interaction challenges in AR.

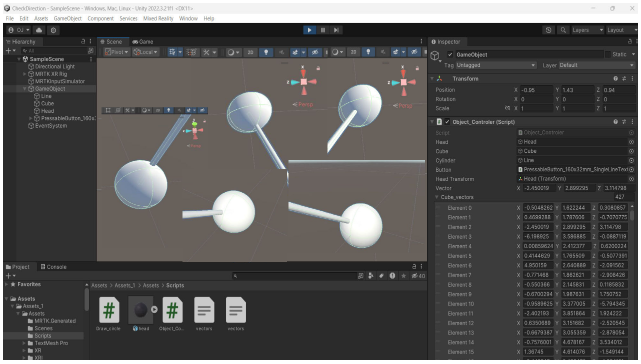

FIGURE 10. Vector data from unity showing interaction points and quadrants for empirical validation. Each vector represents a user's interaction within the AR environment, categorized into different spatial quadrants.

TABLE 5. Weighted average task difficulty ratings for F, L, R, and B series targets based on user feedback.

F series		L series		R series		B series	
Target	WAD	Target	WAD	Target	WAD	Target	WAD
F1	2.38	L1	3.14	R1	2.86	B1	3.57
F2	2.85	L2	3.36	R2	3.43	B2	3.71
F3	2.50	L3	3.43	R3	3.57	B3	3.86
F4	4.35	L4	3.34	R4	3.71	B4	4.07
F5	4.21	L5	5.07	R5	5.00	B5	5.36
F6	4.35	L6	5.29	R6	5.36	B6	5.50

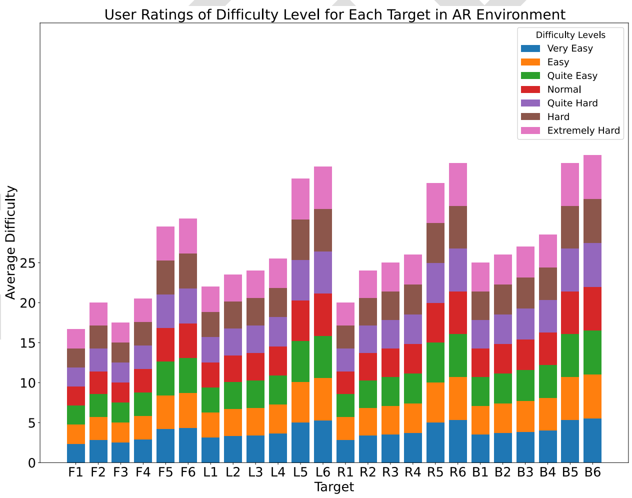

FIGURE 11. This chart presents the collective user feedback from a survey on interaction task difficulty within an augmented reality environment. It summarizes the relative frequency of perceived level of difficulty, offering a consolidated view of user experiences across the spectrum of AR interactions.

VI. DISCUSSION

The findings from this study significantly advance the design of AR interfaces and contribute to the broader field of Human-Computer Interaction (HCI). Integrating head movement and spatial orientation into Fitts' Law provides a more accurate framework for predicting and optimizing interaction task difficulty in AR environments. Applying a genetic optimization algorithm effectively refined model parameters, allowing adaptation across various AR scenarios. Furthermore, using quaternion algebra to handle head rotations addresses limitations in previous models of Fitts' Law.

We structured the interaction space around the user's head based on anatomical planes—frontal, left, right, and back—and subdivided these regions for detailed analysis (Figure 2). Our results reveal varying levels of interaction task difficulty across these regions, with the upper frontal area being particularly challenging due to the complex gaze and head movements required for interactions above the transverse plane. This underscores the importance of ergonomic considerations, especially for objects close to the user's line of sight, as interactions along the vertical axis pose additional challenges.

The analysis further shows that the lower frontal and lateral planes are more accessible to interact with as they align more naturally with head positioning and gaze direction. However, the task difficulty increases in peripheral areas due to the ergonomic constraints of head and neck movement. Factoring in head movement introduces significant ergonomic nuances, with increased interaction task difficulty in initially faced quadrants (Figure 9, 1.51 for V1H1 with head influence).

To optimize the interaction model, we employed a genetic algorithm to adjust parameters such as Lambda (Λ), the strength of head (s), Sigma (σ), and Mu (μ), significantly enhancing the model's performance across spatial quadrants (Figure 3).

Initially, the algorithm started with baseline parameters: ($\Lambda = 3$, $s = 6$, $\sigma = 8$, and $\mu = 4$). The final optimized parameters ($\Lambda = 1.77$, $s = 0.07$, $\sigma = 0.60$, $\mu = 0.02$) achieved a minimized Mean Squared Error (MSE) of 0.98, resulting in an average Level of Difficulty (LoD) reduction by approximately 40%. The first quadrant saw a reduction of about 66.7%, and the fourth quadrant experienced a 40.0% reduction. The second and third quadrants also showed improvements with reductions of approximately 33.3% and 20.0%, respectively, as shown in Figure 15, indicating a more consistent and ergonomic user experience across varying head distances.

This fine-tuning ensures the model's accuracy and user-centricity. Empirical validation, comparing predicted interaction times with actual user performance, showed a strong correlation (Figure 12, R^2 (0.910), Additionally, our analysis of the relationship between task complexity (LoD) and perceived task difficulty (WAD) further validated the model, establishing a critical link between objective task metrics and user experience (Figure 14).

Building on our model's refinement, Figure 16 presents the probability density of task difficulty levels across various user experiences within the AR environment after applying

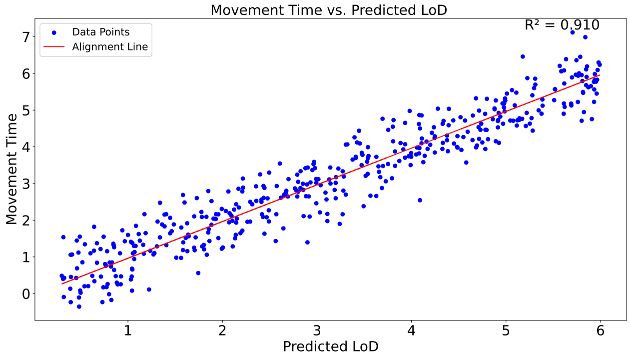

FIGURE 12. Scatter plot showing the correlation between Predicted LoD and actual user movement times, with an R^2 of 0.910 indicating the accuracy of the module.

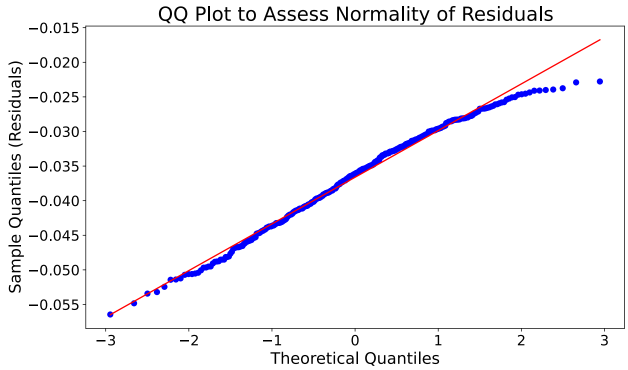

FIGURE 13. QQ Plot of residuals from the model fit, illustrating that the residuals closely follow a normal distribution, supporting the validity of the model's predictions.

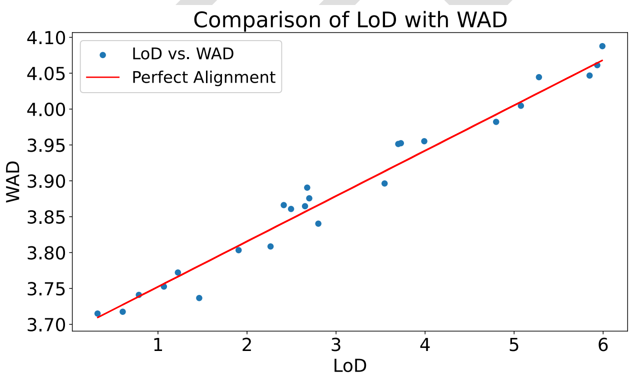

FIGURE 14. Correlation between task complexity (Level of Difficulty, LoD) and user perceived task difficulty (Weighted Average Difficulty, WAD) in an augmented reality Setting.

the optimization algorithms. This figure illustrates the normal distribution of task difficulty, with the mean (μ) signifying the average user-perceived challenge after optimization. The shaded areas represent the 1-sigma (68.27%), 2-sigma (95.45%), and 3-sigma (99.73%) intervals, demonstrating the spread and likelihood of various levels of difficulty encountered. As shown, the fine-tuning of parameters Λ, s,

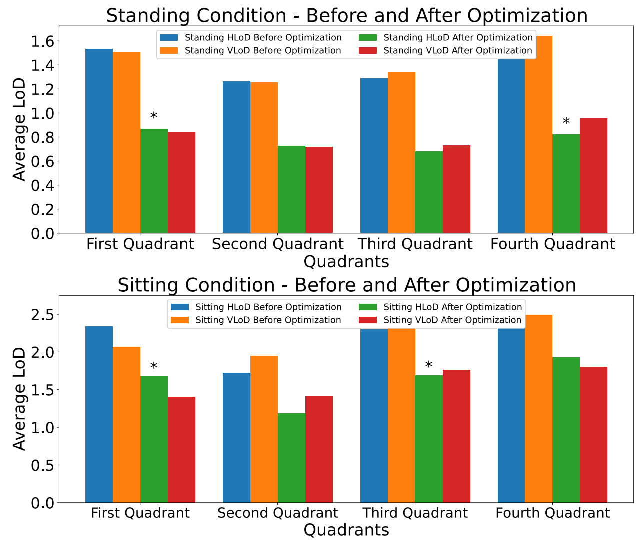

FIGURE 15. LoD comparison by quadrants, pre- and post-optimization.

σ, and μ using the genetic algorithm has not only reduced the mean squared error (MSE) but also tightly concentrated the task difficulty around the optimal point, thereby indicating a more consistent and user-friendly AR experience. The

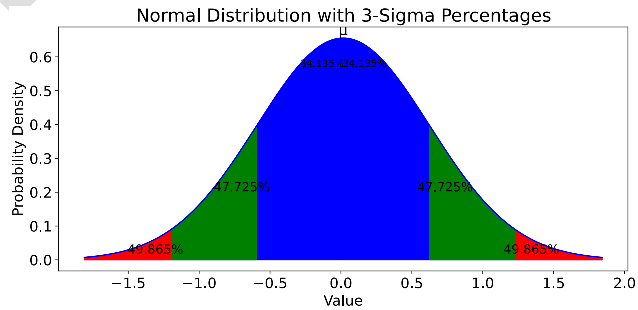

FIGURE 16. The graph illustrates a normal distribution curve with the percentages corresponding to the one, two, and three standard deviation ranges (sigma levels) from the mean μ.

optimized parameters indicate a nuanced model that adapts to the ergonomics of AR interaction, considering the intricate dynamics of user orientation and task complexity. The achieved MSE represents a robust fit of the model to the empirical data, ensuring high confidence in the task difficulty predictions and their alignment with user experience.

In comparison to other established methods, such as the raycasting technique evaluated by Mifsud et al. [28], which achieved an average throughput of 2.63 bits/second and movement times of 1068 ms, our model demonstrated a 40% reduction in interaction task difficulty across various quadrants. While raycasting performs well in AR, our method's inclusion of head movement and ergonomic considerations provides a more tailored interaction model for AR environments, offering consistent reductions in task difficulty across quadrants, particularly in challenging areas like the upper frontal quadrant. These enhancements make our model more suitable for complex AR environments where head orientation plays a significant role.

Additionally, recent work by Wagner et al. [22] highlights the effectiveness of gaze-hand alignment techniques in AR, such as Gaze&Handray, which outperforms raycasting for close-range tasks but struggles with distant targets due to parallax. Our model addresses these limitations, offering a versatile and efficient solution for AR interaction, effectively reducing task difficulty regardless of target distance.

VII. CONCLUSION

The findings of this study, particularly the adaptation of Fitts' Law for AR, have significant implications for the design and optimization of interactive systems beyond AR. This work contributes to a deeper understanding of how Human-Computer Interaction (HCI) principles can be adapted to suit immersive environments, such as Virtual Reality (VR) and Mixed Reality (MR), where user interaction dynamics differ significantly from traditional 2D interfaces.

Moreover, developers could apply the proposed adapted Fitts' Law, which accounts for head movement and spatial orientation, to optimize the placement of objects in the AR environment, providing users with more intuitive and ergonomic interaction. The proposed adapted Fitts' Law-based model demonstrates approximately 40% reduction in interaction task difficulty across all quadrants, resulting in a more ergonomic and intuitive user interface. Our proposed theoretical and experimental methodology provides a framework for performance evaluations and optimization of AR and other user interfaces. To further enhance the impact and applicability of our findings, future research should consider broadening the scope of this study by extending the optimized Fitts's Law model to different AR devices beyond Microsoft Hololens 2, such as Magic Leap, AR-enabled mobile devices, and virtual reality (VR) devices. This expansion would enable a comprehensive comparison of interaction difficulties across different immersive technologies, providing valuable insights into the generalizability and adaptability of the model.

Additionally, real-time measurement of cognitive load (using EEG, eye-tracking, etc.) should be incorporated to see how the task difficulty in AR environments impacts mental workload. This data could further refine the task difficulty metrics used in the study.

ACKNOWLEDGMENT

The authors would like to acknowledge that this article has been written based on the results achieved within the OptiQ project. Views and opinions expressed are however those of they only and do not necessarily reflect those of the European Union or the European Research Executive Agency (REA–granting authority). Neither the European Union nor the granting authority can be held responsible for them.

REFERENCES

[1] A. Y. C. Nee and S. K. Ong, *Springer Handbook of Augmented Reality*. Cham, Switzerland: Springer, 2023.

[2] O. J. Nwobodo, K. Wereszczynski, and K. Cyran, "Slam methods for augmented reality systems for flight simulators," in *Proc. Int. Conf. Comput. Sci.*, 2023, pp. 653–667.

[3] A. Uriarte-Portillo, M.-B. Ibáñez, R. Zataraín-Cabada, and M.-L. Barrón-Estrada, "Higher immersive profiles improve learning outcomes in augmented reality learning environments," *Information*, vol. 13, no. 5, p. 218, Apr. 2022.

[4] I. S. MacKenzie, "Fitts law," in *The Wiley Handbook of Human Computer Interaction*, vol. 1, 2018, pp. 347–370.

[5] L. D. Clark, A. B. Bhagat, and S. L. Riggs, "Extending Fitts' law in three-dimensional virtual environments with current low-cost virtual reality technology," *Int. J. Hum.-Comput. Stud.*, vol. 139, Jul. 2020, Art. no. 102413.

[6] E. Triantafyllidis and Z. Li, "The challenges in modeling human performance in 3D space with Fitts' law," in *Proc. Extended Abstr. CHI Conf. Human Factors Comput. Syst.*, May 2021, pp. 1–9.

[7] O. J. Nwobodo, G. S. Kuaban, T. Kukuczka, K. Wereszczyński, and K. Cyran, "Analysis of marker and slam-based tracking for advanced augmented reality (AR)-based flight simulation," in *Proc. Int. Conf. Comput. Sci.*, 2024, pp. 208–222.

[8] A. Zable, L. Hollenberg, E. Velloso, and J. Goncalves, "Investigating immersive virtual reality as an educational tool for quantum computing," in *Proc. 26th ACM Symp. Virtual Reality Softw. Technol.*, Nov. 2020, pp. 1–11.

[9] C. Zhang, X. Li, F. Gao, F. Zhou, and L. Xu, "An experimental research on the directivity of Fitts' law in human-computer interaction," in *Proc. IEEE Int. Conf. Prog. Informat. Comput. (PIC)*, Dec. 2015, pp. 226–229.

[10] P. Chakraborty and S. Yadav, "Applicability of Fitts' law to interaction with touchscreen: Review of experimental results," *Theor. Issues Ergonom. Sci.*, vol. 24, no. 5, pp. 532–546, Sep. 2023.

[11] L. Sambrooks and B. Wilkinson, "Comparison of gestural, touch, and mouse interaction with Fitts' law," in *Proc. 25th Austral. Computer-Human Interact. Conf. Augmentation, Appl., Innov., Collaboration*, Nov. 2013, pp. 119–122.

[12] R. Jiang and Z. Gu, "Current theoretical developments and applications of fitts? law: A literature review," in *Proc. Int. Conf. Ergonom. Design*, 2019, pp. 753–760.

[13] S. García-Vergara and A. M. Howard, "Three-dimensional fitt's law model used to predict movement time in serious games for rehabilitation," in *Proc. 6th Int. Conf.*, 2014, pp. 287–297.

[14] I. S. MacKenzie and W. Buxton, "Extending Fitts' law to two-dimensional tasks," in *Proc. SIGCHI Conf. Human Factors Comput. Syst. CHI*, 1992, pp. 219–226.

[15] J. Accot and S. Zhai, "Refining Fitts' law models for bivariate pointing," in *Proc. SIGCHI Conf. Human Factors Comput. Syst.*, Apr. 2003, pp. 193–200.

[16] A. Murata and H. Iwase, "Extending Fitts' law to a three-dimensional pointing task," *Human Movement Sci.*, vol. 20, no. 6, pp. 791–805, Dec. 2001.

[17] T. Grossman, D. Wigdor, and R. Balakrishnan, "Multi-finger gestural interaction with 3D volumetric displays," in *Proc. ACM SIGGRAPH Papers*, Jul. 2005, pp. 931–931.

[18] Y. Cha and R. Myung, "Extended Fitts' law for 3D pointing tasks using 3D target arrangements," *Int. J. Ind. Ergonom.*, vol. 43, no. 4, pp. 350–355, Jul. 2013.

[19] I. Schuetz, T. S. Murdison, K. J. MacKenzie, and M. Zannoli, "An explanation of Fitts' law-like performance in gaze-based selection tasks using a psychophysics approach," in *Proc. CHI Conf. Human Factors Comput. Syst.*, May 2019, pp. 1–13.

[20] X. Lou, X. A. Li, P. Hansen, and P. Du, "Hand-adaptive user interface: Improved gestural interaction in virtual reality," *Virtual Reality*, vol. 25, no. 2, pp. 367–382, Jun. 2021.

[21] G. Liu, S. Lv, X. Wang, and X. Sun, "Performance of the rotation gesture based on electrostatic tactile feedback devices," *Interacting Comput.*, vol. 33, no. 5, pp. 511–521, Jul. 2021.

[22] U. Wagner, M. N. Lystbak, P. Manakhov, J. E. S. Grønbak, K. Pfeuffer, and H. Gellersen, "A Fitts' law study of gaze-hand alignment for selection in 3D user interfaces," in *Proc. CHI Conf. Human Factors Comput. Syst.*, Apr. 2023, pp. 1–15.

[23] A. J. Haskins, J. Mentch, T. L. Botch, and C. E. Robertson, "Active vision in immersive, 360° real-world environments," *Sci. Rep.*, vol. 10, no. 1, p. 14304, Aug. 2020.

[24] J. Delmerico, R. Poranne, F. Bogo, H. Oleynikova, E. Vollenweider, S. Coros, J. Nieto, and M. Pollefeys, ''Spatial computing and intuitive interaction: Bringing mixed reality and robotics together,'' *IEEE Robot. Autom. Mag.*, vol. 29, no. 1, pp. 45–57, Mar. 2022.

[25] R. Kazemi and S. C. Lee, ''Human factors/ergonomics (HFE) evaluation in the virtual reality environment: A systematic review,'' *Int. J. Hum.-Comput. Interact.*, vol. 40, no. 17, pp. 4533–4549, Sep. 2024.

[26] R. Alazrai, Y. Mowafi, and C. S. George Lee, ''Anatomical-plane-based representation for human–human interactions analysis,'' *Pattern Recognit.*, vol. 48, no. 8, pp. 2346–2363, Aug. 2015.

[27] A. Switołski, H. Josiłski, A. Michalczuk, and K. Wojciechowski, ''Quaternion statistics applied to the classification of motion capture data,'' *Expert Syst. Appl.*, vol. 164, Feb. 2021, Art. no. 113813.

[28] D. M. Mifsud, A. S. Williams, F. Ortega, and R. J. Teather, ''Augmented reality Fitts' law input comparison between touchpad, pointing gesture, and raycast,'' in *Proc. IEEE Conf. Virtual Reality 3D User Interface Abstr. Workshops (VRW)*, Mar. 2022, pp. 590–591.

ONYEKA JOSEPHINE NWOBODO received the Bachelor of Engineering (B.Eng.) degree in computer engineering from Enugu State University of Science and Technology Enugu, Nigeria, in 2008, and the master's (M.Sc.) degree in computer science from the University of Silesia in Katowice, in 2020. She is currently pursuing the doctoral (Ph.D.) degree with the Department of Computer Graphics, Vision, and Digital Systems, Faculty of Automatic Control, Electronics, and Computer Science, Silesian University of Technology.

She participated in two EU-funded research projects: One is WrightBros, which focused on developing an augmented reality flight simulator for pilot training, and the later is OptiQ, which concentrates on non-standard data and image processing in advancing quantum computing. Her professional interests include augmented reality, virtual reality, simultaneous localization mapping (SLAM), computer vision, and image processing.

KAMIL WERESZCZYŃSKI received the Ph.D. degree in computer science from the Silesian University of Technology Gliwice, Poland, in 2022. He is a Researcher specializing in quantum computing and artificial intelligence. Currently, he is the Head of the Quantum Computing Laboratory, Silesian University of Technology. His expertise spans quantum information theory, deep learning, statistical learning, object recognition, manifold (mathematics), manifold learning, and computer vision.

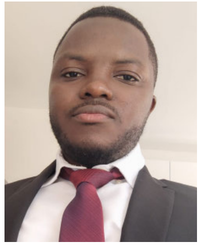

GODLOVE SUILA KUABAN received the B.Eng. degree in electrical and electronics engineering from the University of Buea, Cameroon, in 2014, with a specialty in telecommunications, and the M.Sc. degree in automatic control, robotics, electronics, telecommunication, and computer science interdisciplinary studies and specialized in computer science and the Ph.D. degree in telecommunications and technical computer science from the Silesian University of Technology, Gliwice, Poland, in 2017 and 2017, respectively.

From 2017 to 2023, he was a Research Assistant with the Institute of Theoretical and Applied Informatics, Polish Academy of Science (IITiS-PAN), Gliwice. He is currently an Assistant Professor with IITiS-PAN. His research interests include computer systems modeling and performance evaluations. Specifically, modeling and evaluations of SDN and IoT networks and energy performance of green networks (e.g., IoT and cellular mobile networks, linear wireless sensor networks). He has participated in six EU-funded research grants: three in IoT security, one in building IoT laboratory testbed, one in developing online education resources on assembly language programming, and one on reliable electronics for tomorrow's active systems. Also, he received the Best Paper Award at the 31st International Symposium on the Modeling, Analysis, and Simulation of Computer and Telecommunication Systems (MASCOTS 2023) in Stony Brook, NY, USA (published by IEEE).

PRZEMYSŁAW SKUROWSKI received the M.Sc. and Ph.D. degrees in computer science from the Department of Computer Graphics, Vision, and Digital Systems, Faculty of Automatic Control, Electronics, and Computer Science, Silesian University of Technology, in 2000 and 2007, respectively. He is currently an Assistant Professor with the Department of Computer Graphics, Vision, and Digital Systems, Faculty of Automatic Control, Electronics, and Computer Science, Silesian University of Technology. His professional interests include motion capture, visual information systems, and human-centric image and signal processing.

KRZYSZTOF ADAM CYRAN is currently a Professor with the Department of Computer Graphics, Vision, and Digital Systems, Faculty of Automatic Control, Electronics, and Computer Science, Silesian University of Technology. Since 2011, he has been the Director of the Virtual Flight Laboratory (VFL), SUT, Gliwice, Poland. He has been the coordinator and/or principal investigator in many EU-funded projects, including the OptiQ project (non-standard data and image processing from nonlinear optics to quantum computing, from 2023 to 2026, the WrightBroS project (Working in a Collaborative Factory of the Flight Simulators Branch of RISE), from 2019 to 2023, RFSC project Telerescuer (System for Virtual TELEportation of RESCUER for inspecting coal mine areas affected by catastrophic events), from 2014 to 2017. His professional interests include pattern recognition, image processing, optical information processing, smart sensors, signal processing, photonics, quantum computing, man-machine interactions, flight simulators, augmented reality, virtual reality, machine learning, and artificial intelligence.